ELSEVIER

Biophysical Chemistry 73 (1998) 189–203

Biophysical Chemistry

Molecular orbital study of porphyrin–substrate interactions in cytochrome P450 catalysed aromatic hydroxylation of substituted anilines

Olga Zakharieva[a,b], Michael Grodzicki[c], Alfred X. Trautwein[c,*], Cees Veeger[a], Ivonne M.C.M. Rietjens[a]

[a] *Department of Biochemistry, Agricultural University, Dreijenlaan 3, 6703 Wageningen, The Netherlands*
[b] *Physical Faculty, University of Sofia, Sofia 1126, Bulgaria*
[c] *Institute of Physics, Medical University Lübeck, 23538 Lübeck, Germany*

Received 6 August 1997; received in revised form 12 January 1998; accepted 2 February 1998

Abstract

The reaction mechanism for the primary reaction step of the hydroxylation of 3-fluoro-6-methylaniline, attacked at different positions (oxygen attack across a C–C bond and direct attack at positions *para* and *ortho* with respect to the NH_2-group) catalysed by a high-valent ferryl-oxo porphyrin a_{2u}-cation complex with H_3CS^- as an axial ligand, has been investigated on the basis of electronic structure calculations in local spin-density approximation. Non-repulsive potential curves are obtained only in cases of direct attack at the *para*- and *ortho*-positions with respect to NH_2, but not for epoxide formation. Comparing the potential curves for the hydroxylation at the positions *para* and *ortho* to the NH_2-group, an attack at the *para*-position is more likely. The relative orientation of the substrate towards the porphyrin is essentially determined by the interaction between the substituents of the substrate and the porphyrin. Consequently, different geometrical orientations of the substrate are obtained for hydroxylation at the *para*- and *ortho*-positions. In both cases of direct attack the substrate plane is not parallel to the porphyrin plane. The decisive role of sulphur in the hydroxylation is demonstrated by the participation of the S(3p)-orbitals in all molecular orbitals involved in the reaction.

Keywords: Cytochrome P450; Molecular orbital calculations; Hydroxylation

* Corresponding author.

0301-4622/98/$19.00
PII S0301-4622(98)00111-2

1. Introduction

The high-valent ferryl-oxo porphyrin cation radical complex $[PorFe(IV)O]^+$, also denoted as compound I, is generally taken as the common intermediate in haem-based (per)oxidations and monooxygenations. It is moreover assumed that a compound-1-like intermediate represents also the active species involved in reactions mediated by cytochrome P450. Since cytochromes P450 are key enzymes of biological oxidations of a wide variety of xenobiotic compounds, a detailed understanding of the mechanism of hydroxylation is of continuing interest [1–18]. Most of these investigations have focused on identifying possible reaction pathways and the factors that determine the substrate–porphyrin interaction. As to the hydroxylation of aromatic substrates, a long lasting dispute concerns the involvement of epoxide intermediates in the pathway leading to formation of phenolic metabolites. The original suggestion that aromatic hydroxylation proceeds via epoxide intermediates [19–21] has been challenged since the formation of meta-hydroxylated metabolites from a halobenzene can not proceed through epoxide intermediates. Studies on the hydroxylation of deuterated bromobenzenes [22] and chlorobenzenes [3] provide evidence for pathways leading to the formation of phenolic metabolites from halogenated benzene derivatives without epoxide and/or cyclohexadienone intermediates. Rizk and Hanzlik arrived at similar conclusions on the basis of results proving the absence of any deuterium loss upon conversion of deuterated [3,5-$^2H_2$]-4-iodoanisole to 2-methoxy-5-iodophenol [23]. Finally, the regioselectivity of the aromatic hydroxylation of fluorobenzenes has satisfactorily been described within the frame of frontier orbital theory [5]. This indicates that the site of attack by the electrophilic ferryl-oxo group of cytochrome P450 is the site of hydroxylation. However, unlike the aromatic hydroxylation of fluorobenzenes, the amino substituted benzene derivatives exhibit systematic deviations between observed and calculated regioselectivities [9].

In order to understand the origin of these deviations, molecular orbital calculations explicitly including the haem system as well as the substrate will be necessary. In a previous paper [1] we have demonstrated that hydroxylation reactions can adequately be described by a molecular orbital treatment in local spin-density approximation [24,25], since the reaction mechanism is dominated by orbital interactions. Here we extend these investigations to the non-symmetric substrate 3-fluoro-6-methylaniline, in order to examine to which extent the substituents of the substrate influence the porphyrin–substrate interaction and determine the preferential substrate orientation.

In the particular case of anilines, several mechanisms for the cytochrome P450 aromatic hydroxylation have been proposed [6,7,18], such as direct attack at the nitrogen of the amino group by either hydrogen abstraction or single-electron transfer to cytochrome P450, or direct attack at one of the carbon atoms of the benzene ring leading to the formation of aminophenols.

The aim of this paper is to determine factors that may contribute to the regioselectivity and to the orienting interactions between the aniline derivative and the activated ferryl-oxo porphyrin cofactor of cytochromes P450, as well as to elucidate the orbital interactions during the primary reaction step and the mechanism of the Fe–O bond rupture. To this end, three possible primary reaction steps for the hydroxylation of 3-fluoro-6-methylaniline are investigated in the present paper, namely direct attack at the carbon atoms *para* and *ortho* with respect to the amino group, and epoxide formation. The haem system as well as the substrate are explicitly included in the calculations.

2. Procedures and methods

It has recently been shown that the energetics of chemical reactions can theoretically be described by local density functional methods with results comparable to or even better than those of Hartree–Fock calculations including many-body perturbation corrections up to fourth order [26,27]. Those calculations were performed by defining a certain reaction coordinate, followed by full geometry optimization along that coordinate, and proving the transition state by vibrational

analysis. However, an analogous procedure would be prohibitive in the case of the reactions investigated in this work because the whole system consisting of substrate and ferryl-oxo porphyrin contains 60 atoms with 176 valence orbitals, and it is an open-shell system requiring spin-polarized calculations. Moreover, a large number of iterations is generally needed until convergence of the electron density is reached, because the occupied and empty orbitals are energetically not well separated from each other. For these reasons, a full geometry optimization along the reaction coordinate is not feasible, so that the main purpose of this investigation consists in understanding, at least qualitatively, the changes that the two interacting systems undergo during the process of hydroxylation and how the final state is reached. Previous calculations on the hydroxylation of monofluorobenzene by a ferryl-oxo porphyrin have shown that valuable insight into the reaction mechanisms can be achieved even without full geometry optimization along the chosen reaction coordinate [1].

2.1. Geometrical assumptions

Since gas-phase geometries for the substrate molecules (3-fluoro-6-methylaniline and 3-fluoroaniline) are not available, their structures have been determined by ab-initio calculations using an STO-3G basis set [28]. The dihedral angle between the planes of benzene and NH_2 is 61°. The geometrical structure of the compound I analogue is the same as in the previous calculations [1]. The atomic positions of the porphyrin core are derived [29] from crystal structure data of free base porphine [30] by taking the average values of equivalent bond distances and bond angles in order to preserve the fourfold symmetry. The iron is placed at the center of the porphyrin ring, resulting in an iron–nitrogen distance of 204 pm. Analogous calculations are also performed with a shorter Fe–N distance of 200 pm to resemble more closely the situation in metalloporphyrins [31] and to check the effect of the Fe–N bond length. The oxo–iron distance is assumed to be 165 pm, consistent with structural data derived from EXAFS [32]. The geometry and orientation of the H_3CS^- anion, modelling the axial cysteinate ligand, are taken from the crystal structure of the haemoprotein domain of P450BM-3 [33] with the iron–sulphur distance set to 231 pm. The sulphur atom is tilted by 6° out of the porphyrin normal direction towards the positive x-axis. For reasons of comparison with our previous calculations [1], the electronic structure of the compound 1 analogue is taken as the $A^{\bullet}_{2u}$-cationic state with parallel coupling of the ferryl iron spin ($S = 1$) and the a_{2u}-radical spin ($S' = 1/2$). The notation a_{2u} refers to D_{4h} symmetry although the actual symmetry of the system is lower.

In the course of the reaction both the substrate and the porphyrin undergo deformations. As in our previous calculations [1] the Fe–O distance is increased during the reaction stepwise from 165 pm to 185 pm to account for the weakening of the Fe–O bond along the reaction pathway while the Fe–S distance is kept constant, and the porphyrin core is assumed to remain planar. The substrate is also deformed stepwise during the reaction so that the transition state geometry of the intermediates, as calculated by Korzekwa [2] is obtained, namely:

(i) In the case of direct attack at the C_4-position *para* with respect to the amino group, the next-neighbour bonds of the carbon atom under attack (C_4) are elongated stepwise, C_4–C_3 from 139.4 pm to 152.5 pm and C_4–C_5 from 138.0 pm to 152.5 pm (cf. Fig. 1 for the numbering of atoms).

Additionally, the C_4–H_{14} bond length is increased stepwise from 108.1 pm to 113.6 pm, and the hydrogen atom is pushed out of the substrate plane so that the carbon atom under attack approaches a state being near to tetrahedral symmetry.

(ii) In the case of direct attack at the C_2-position *ortho* with respect to the amino group, the next-neighbour bonds C_2–C_1 and C_2–C_3 are elongated stepwise from 139.5 pm to 152.5 pm and from 138.7 pm to 152.5 pm, respectively. Also the C_2–H_{12} bond length is increased stepwise from 108.1 pm to 113.6 pm, and the hydrogen

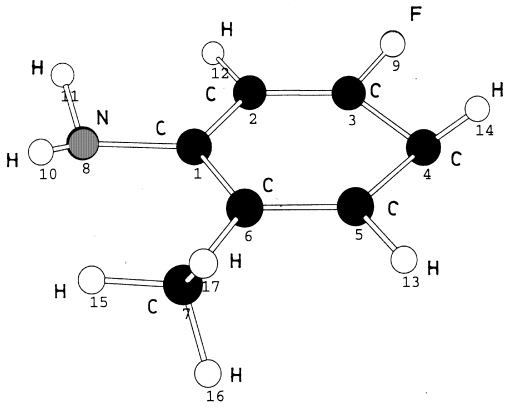

Fig. 1. Numbering scheme for the atoms of the deformed 3-fluoro-6-methylaniline substrate.

atom is pushed out of the substrate plane so that the carbon atom under attack approaches a state being close to tetrahedral symmetry.

(iii) In case of epoxide formation as the primary reaction step, where the oxygen attack occurs across the C_4–C_5 bond, this bond length is elongated along the reaction from 138.0 pm to 152 pm, the C_4–H_{14} and C_5–H_{13} bond lengths are increased from 108.1 pm to 113.6 pm, and both hydrogen atoms are moved out of the substrate plane in order to simulate sp^3 hybridization state for both carbon atoms in the transition state [2]. In addition to these model assumptions, the bond lengths of C_4 and C_5 with the neighbouring C atoms are increased to 152 pm.

The assumed reaction coordinate is the C–O distance representing the bond to be formed during hydroxylation. The geometry optimization along this reaction coordinate will in general be restricted to the variation of the relative orientation of the deformed substrate with respect to the porphyrin.

2.2. Theoretical method

The molecular orbital calculations have been performed within the local density approximation [34–36] by the self-consistent charge (SCC)-Xα method [24]. This approach is based on the frozen core approximation and a model potential for the valence electron density that enables the analytical evaluation of all angular parts of the matrix elements and leaves only one-dimensional numerical integrations for the exchange-correlation potential. The population analysis is performed by numerical integration of the electron density within appropriately chosen atomic spheres. As a whole, the SCC-Xα code is an order of magnitude faster than the Xα option of GAUSSIAN94 and requires substantially less memory space. For these reasons this method is particularly suited for describing the electronic properties of large molecules containing transition metal atoms as shown by several applications to systems of biological relevance [1,29,37–39].

3. Optimization of the substrate orientation

In contrast to the previously investigated monofluorobenzene, 3-fluoro-6-methylaniline does not exhibit any symmetry due to the substituents that, in addition, may interact with the porphyrin and influence the relative orientation of the substrate. Therefore a reasonable guess for the reaction pathway is considerably more complicated than in the case when symmetric substrates are concerned. Optimization of the geometrical orientation of the substrate relative to the porphyrin will be described in detail for the three cases under study namely attack at carbon in position *para* with respect to the amino group, attack at carbon in position *ortho* to the amino group as well as oxygen attack across a C–C bond. An orientation of the substrate with the NH_2 group towards the oxygen yields higher total energies than an orientation with the carbon atom directed towards the oxygen, and is therefore less probable. An orientation with the hydrogens of the amino group directed away from the porphyrin plane is energetically more favourable than the reversed positions of the amino hydrogens. Since initial H abstraction from the amino group requires the latter orientation this is another indication that such a primary reaction step is less probable.

In our search for the most suitable substrate–porphyrin orientation, supporting the hydroxyla-

tion reaction, several rotations of the substrate around axes parallel to *x*-, *y*- and *z*-axis have been performed.

3.1. Hydroxylation reaction at the para-position

Starting with the hydroxylation of 3-fluoro-6-methylaniline at the carbon position (C_4) *para* with respect to the amino group, we follow the procedure described in our previous calculations for the hydroxylation of benzene and fluorobenzenes [1] and assume in a first step, that the substrate molecule approaches the porphyrin along the *x*-axis with its molecular plane parallel to the porphyrin plane, defined as the (x,y)-plane. The obtained interaction between substrate and porphyrin is repulsive in the whole range of C–O distances between 245 pm and 153 pm (data not shown).

Next, a stepwise rotation of the substrate around the *z*-axis at a fixed C–O distance of 226 pm is performed so that the parallel orientation of the molecular plane with respect to the porphyrin is preserved. A rotational barrier of 4 kcal/mol derived from the differences in the binding energies is obtained with the minimum for an orientation where the substrate approaches the porphyrin along the negative *x*-axis, corresponding to a position trans to the sulphur atom of the axial ligand. These differences in the binding energies are influenced by the asymmetry in the spin and charge distribution within the porphyrin nitrogen atoms arising from the sulphur tilted by 6° out of the porphyrin normal direction towards the positive *x*-axis as well as by the geometrical orientation of the methyl group of the SCH_3^- axial ligand. The calculation of the potential curve with this optimized orientation of the substrate still yields a repulsive interaction for C–O distances between 245 pm and 153 pm.

Furthermore, the substrate is rotated around an axis through C_4 parallel to the *y*-axis from 0° to 60° in steps of 5°, while the position of H_{14} is kept constant. Again, a repulsive interaction is obtained for every single angle in the C–O distance range between 245 pm and 153 pm. The most stable orientation of the substrate with respect to the porphyrin is found for an angle α of 45° (Fig. 2) yielding a strong relative stabilization of approx. 100 kcal/mol. This stabilization reflects the expected tendency of the substituents to move away from the haem surface, and is taken as an indication of approaching the correct geometrical orientation. Moreover, computation of the repulsive Coulomb interactions between the N-, C- and F-atoms of the substituents with O, S and the N_p-atom of the porphyrin ring closest to the substrate reveals significant diminishing of these repulsions with the above-mentioned rotation. This last rotation causes a decrease of the angle between the substrate plane and the C_4–H_{14} bond direction, and leads to repulsive covalent interactions of H_{14} with the neighbouring carbon atoms and the fluorine of the aromatic ring. Therefore the position of H_{14} is optimized separately so that this repulsion is reduced while, at the same time, the approximately tetrahedral angle between O, C_4 and H_{14} (cf. Fig. 2) is preserved as much as possible, in order to favour the formation of the new C–O bond. Rotations of H_{14} are performed around the axis through C_4 parallel to the *y*-axis from 0° to 20° in steps of 5°. Under these conditions, potential curves are calculated which become attractive for C–O distances shorter than approx. 180 pm (See Fig. 3). The lowest energy barrier is obtained for a rotation angle of 10°. Additional rotations around an axis through C_4 parallel to the *x*-axis yield higher energies and are less probable. Practically the same results are obtained for the hydroxylation at the *para* position for the porphyrin model with the shorter Fe–N bond distance of 200 pm. The results are available as supplementary material (Fig. S1).

To sum up, in case of hydroxylation at a position *para* with respect to the NH_2 group, the substrate approaches the haem group along the negative *x*-axis, the dihedral angle between the plane of the substrate and the porphyrin plane is 45°, and H_{14} is rotated by 10° around an axis through C_4 parallel to the *y*-axis (Fig. 2).

3.2. Hydroxylation reaction at the ortho position

The optimization of the reaction pathway for the direct attack of the substrate at the carbon

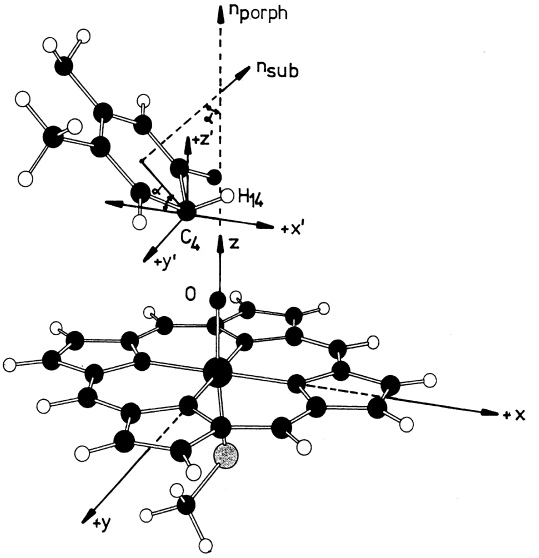

Fig. 2. Geometrical arrangement of the substrate–porphyrin system for the hydroxylation at the position *para* with respect to the NH_2 group. x', y', z' is the translated coordinate system with C_4 as the origin. n_{porph} denotes the normal direction of the porphyrin plane and n_{sub} denotes the normal direction of the substrate plane. The axis through the iron and sulphur is tilted by an angle of 6° out of the porphyrin normal direction (z-axis).

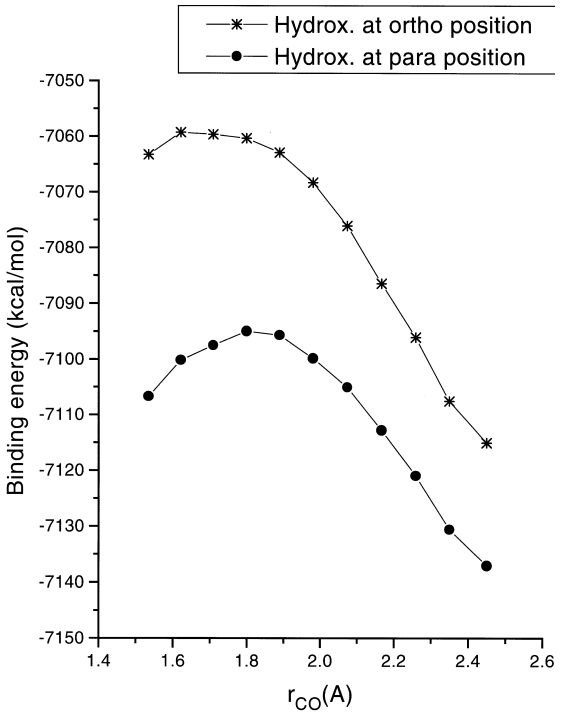

Fig. 3. Changes in binding energies of the substrate–porphyrin system for the hydroxylation of 3-fluoro-6-methylaniline for *para* and *ortho* sites of attack as a function of the C–O distance.

position (C_2) *ortho* with respect to the amino group follows the same strategy namely the substrate approaches the porphyrin along the negative x-axis, rotations are performed around the axis parallel to the y-axis through C_2 up to 60° in steps of 5°, where H_{12} is rotated first by 10° around this axis and is then kept fixed in this position. As in the case of the attack at the *para*-position, the most stable orientation is obtained for a rotational angle of 45°. However, the calculated potential curves are repulsive for all these investigated orientations, and the whole system is approx. 30 kcal/mol less stable than in case of the direct attack at the *para*-position (data not shown).

Further rotations of the substrate around an axis through C_2 parallel to the x-axis are performed for angles up to 40° in steps of 5°. Small angles of this additional rotation up to 20° stabilize the system as a whole, while for larger angles the porphyrin–substrate system is again destabilized. Only at a rotation angle of 10° a non-repulsive potential curve is obtained (Fig. 3).

This result shows that it is energetically favourable for the system to keep the NH_2- and CH_3-groups apart from the porphyrin. At the same time, however, fluorine is coming too close to the haem plane for larger rotational angles, so that the repulsive Coulomb interactions with the porphyrin skeleton yield an unfavourable conformation. Hence, the small rotational angle of 10° is a compromise between: (i) the repulsive Coulomb interactions between N of the NH_2 group and C of the CH_3 group with the porphyrin skeleton; and (ii) the corresponding ones between F and the porphyrin skeleton. This is the only geometrical orientation which, in our search, leads to an attractive substrate–porphyrin interaction for C–O-distances below 160 pm, 20 pm shorter than in the case of the hydroxylation at a position *para* with respect to the NH_2 group (Fig. 3).

Summarizing, in the case of hydroxylation at a position *ortho* with respect to the NH_2 group the substrate approaches the porphyrin along the negative *x*-axis. The dihedral angle between the plane of the substrate and the plane of the porphyrin is 45°. Additionally, the substrate is rotated by 10° around an axis through C_2 parallel to the *y*-axis. In contrast to the hydroxylation of monofluorobenzene [1], the optimized geometrical orientation for the hydroxylation at the *para*- and *ortho*-positions depends significantly on the site of attack. The orientation is determined by repulsive interactions between the substituents of the substrate and the porphyrin but not by the dipole–dipole interaction between the substrate and the porphyrin. This can be concluded from the fact that the dipole–dipole interaction between the substrate and the porphyrin is not favourable because the orientation of the dipole moments is approximately antiparallel in the optimized geometry. This indicates that the weak dipole–dipole interaction does not determine the substrate orientation towards the porphyrin.

3.3. Epoxide formation

As an alternative primary reaction step, epoxide formation is investigated with the oxygen attack occurring across the C_4–C_5 bond. An approach of the substrate along the negative *x*-axis with parallel orientation of the plane of the substrate and the plane of the porphyrin yields repulsive interactions for C–O-distances down to 153 pm. Additionally, the whole system is considerably less stable in comparison with the direct attack at the *para*-position. When the substrate is rotated around an axis through C_4 and C_5, being parallel to the *y*-axis, an overall stabilization of the system is obtained, but the substrate–porphyrin interaction remains repulsive in the whole range of C–O-distances between 245 pm and 153 pm.

The hydroxylation via epoxide formation of the simpler substrate 3-fluoroaniline has also been investigated. Exploring the same orientations as described above, only repulsive interactions are found. Altogether, the repulsive potential curves and the strong destabilization of the whole system compared with the direct attack at the carbon position *para* or *ortho* with respect to the amino group may be interpreted as a strong indication that for both substrates, 3-fluoro-6-methylaniline and 3-fluoro-aniline, the hydroxylation via, epoxide formation as a primary reaction step is unlikely. These results supply an additional argument in the long-lasting dispute about cytochrome P450 catalysed aromatic hydroxylation, namely, that also a non-arene mechanism (without formation of epoxide intermediates as a primary reaction step) is possible [3,22,40,41].

3.4. Final reaction pathway

In summary, varying the place of attack as well as the orientation of the substrate towards the catalytic center, yields the following results:

1. hydroxylation via epoxide formation as a primary reaction step is unlikely;
2. an attractive interaction is obtained only in two cases, namely for the direct attack at the *para*- and at the *ortho*-position with respect to NH_2 (Fig. 3); and
3. hydroxylation at the *ortho*-position with respect to NH_2 is less favourable compared with the *para*-position in view of the distinct destabilization of the whole system by approx. 30 kcal/mol, the shorter C–O distance where the interaction becomes attractive and the difference in the relative height of the energy barriers of approx. 13 kcal/mol (Fig. 3). It is interesting to note that this finding of the preferential *para*- over *ortho*-hydroxylation is in qualitative accordance with results [9] obtained from the in vivo biotransformation of the 3-fluoro-6-methylaniline to aromatic ring hydroxylated products by cytochrome P450.

4. Electronic structure

4.1. Charge and spin distribution in the $[PorFe(IV)O]^+$–substrate complexes

In order to obtain insight into the reaction mechanism, the changes in the charge- and spin-

Table 1
Changes of effective charges for the reaction of 3-fluoro-6-methylaniline with the cysteinate-type coordinated $Por^+Fe(IV)O$ cation radical complex (attack on *para*-position with respect to NH_2)

r_{OC}	Porphyrin				Substrate				
	Q(Fe)	Q(O)	Q(S)	$Q(N_3)$	$Q(C_4)$	$Q(C_3)$	$Q(N_{an})$	Q(F)	Q(sub)[b]
inf[a]	0.840	−0.576	−0.315	−0.180	−0.073	0.087	−0.189	−0.197	0.0
245	0.885	−0.580	−0.310	−0.184	0.019	0.108	−0.189	−0.206	0.067
235	0.885	−0.582	−0.310	−0.185	0.030	0.110	−0.188	−0.206	0.089
226	0.887	−0.584	−0.310	−0.186	0.044	0.112	−0.187	−0.205	0.114
217	0.893	−0.584	−0.309	−0.188	0.061	0.115	−0.185	−0.204	0.145
207	0.902	−0.583	−0.308	−0.190	0.081	0.119	−0.185	−0.203	0.117
198	0.915	−0.581	−0.304	−0.198	0.106	0.122	−0.184	−0.202	0.215
189	0.928	−0.576	−0.299	−0.196	0.130	0.125	−0.183	−0.201	0.252
180	0.939	−0.568	−0.295	−0.199	0.149	0.127	−0.183	−0.201	0.279
171	0.944	−0.559	−0.292	−0.200	0.163	0.127	−0.184	−0.201	0.289
162	0.946	−0.548	−0.292	−0.202	0.171	0.126	−0.184	−0.202	0.288
153	0.946	−0.534	−0.292	−0.202	0.174	0.125	−0.187	−0.203	0.289

[a] Separated systems with deformed structures (see text).
[b] Molecular charge of the substrate.

density distributions along the optimized reaction coordinate for the hydroxylation at *para*- and *ortho*-positions are analysed. The corresponding data are presented in Tables 1–6.

When the substrate moves along the reaction coordinate, an electron flow occurs from the substrate towards the porphyrin (cf. last column of Tables 1 and 2). The substrate becomes partially ionized with a total charge of +0.279 at the C–O distance of 180 pm corresponding to the maximum of the potential curve (hydroxylation at para position).

The charge transfer is higher compared with the hydroxylation of monofluorobenzene [1] because of the electron donating effect of the additional substituents NH_2 and CH_3. Connected with

Table 2
Changes of effective charges for the reaction of 3-fluoro-6-methylaniline with the cysteinate-type coordinated $Por^+Fe(IV)O$ cation radical complex (attack on *ortho*-position with respect to NH_2)

r_{OC}	Porphyrin				Substrate				
	Q(Fe)	Q(O)	Q(S)	$Q(N_3)$	$Q(C_2)$	$Q(C_3)$	$Q(N_{an})$	Q(F)	Q(sub)[b]
inf[a]	0.840	−0.576	−0.315	−0.180	−0.056	0.087	−0.191	−0.197	0.0
245	0.886	−0.585	−0.312	−0.187	0.033	0.109	−0.175	−0.206	0.070
235	0.887	−0.587	−0.312	−0.189	0.045	0.111	−0.173	−0.205	0.118
226	0.889	−0.589	−0.312	−0.190	0.059	0.114	−0.172	−0.205	0.090
217	0.895	−0.589	−0.311	−0.192	0.076	0.118	−0.169	−0.204	0.149
207	0.909	−0.587	−0.310	−0.195	0.095	0.120	−0.166	−0.204	0.180
198	0.917	−0.585	−0.306	−0.198	0.120	0.123	−0.165	−0.203	0.217
189	0.930	−0.580	−0.301	−0.201	0.144	0.125	−0.163	−0.202	0.254
180	0.942	−0.571	−0.297	−0.204	0.164	0.127	−0.162	−0.202	0.280
171	0.948	−0.562	−0.295	−0.206	0.177	0.126	−0.159	−0.202	0.290
162	0.950	−0.551	−0.295	−0.207	0.184	0.124	−0.160	−0.203	0.289
154	0.950	−0.536	−0.295	−0.208	0.188	0.123	−0.160	−0.204	0.290

[a] Separated systems with deformed structures (see text).
[b] Molecular charge of the substrate.

Table 3
Changes of overlap populations for the reaction of 3-fluoro-6-methylaniline with the cysteinate-type coordinated Por^+ Fe(IV)O cation radical complex (attack on *para*-position with respect to NH_2)

r_{OC}	Fe=O	Fe–S	O–C_4	Fe–N_3	C_4–H	C_1–N
inf[a]	0.408	0.209	—	0.220	0.717	0.822
2.449	0.400	0.214	0.021	0.223	0.714	0.823
2.350	0.396	0.214	0.033	0.223	0.715	0.824
2.260	0.390	0.215	0.051	0.223	0.716	0.824
2.167	0.381	0.216	0.080	0.222	0.718	0.825
2.074	0.368	0.217	0.123	0.222	0.719	0.825
1.981	0.350	0.218	0.187	0.222	0.719	0.826
1.890	0.330	0.220	0.269	0.221	0.717	0.826
1.800	0.309	0.222	0.363	0.221	0.711	0.826
1.710	0.291	0.223	0.457	0.221	0.699	0.825
1.622	0.277	0.223	0.547	0.221	0.682	0.824
1.535	0.222	0.222	0.632	0.221	0.659	0.823

[a] Separated systems with deformed structures (see text).

Table 4
Changes of overlap populations for the reaction 3-fluoro-6-methylaniline with the cysteinate-type coordinated Por^+ Fe(IV)O cation radical complex (attack on *ortho*-position with respect to NH_2)

r_{OC}	Fe=O	Fe–S	O–C_4	Fe–N_3	C_2–H	C_1–N
inf[a]	0.408	0.209	—	0.220	0.717	0.837
2.449	0.400	0.215	0.023	0.223	0.717	0.837
2.350	0.396	0.215	0.036	0.223	0.718	0.838
2.260	0.390	0.215	0.054	0.223	0.719	0.839
2.167	0.381	0.216	0.083	0.223	0.720	0.839
2.074	0.367	0.217	0.125	0.223	0.722	0.839
1.981	0.349	0.219	0.188	0.222	0.722	0.841
1.890	0.329	0.221	0.270	0.222	0.720	0.842
1.800	0.307	0.222	0.363	0.223	0.714	0.842
1.710	0.290	0.223	0.456	0.221	0.703	0.842
1.622	0.276	0.224	0.546	0.221	0.686	0.841
1.535	0.263	0.223	0.631	0.222	0.663	0.841

[a] Separated systems with deformed structures (see text).

this electron flow the following changes in the charge- and spin-density distribution of the haem and the substrate occur. The positive charge of Fe gradually increases (cf. Table 1) approaching the value for the final reaction product when the oxygen is completely separated from the porphyrin. The negative charge of oxygen undergoes minor changes, so that only a small part of the electron flow is transferred directly to the oxygen, while the remaining part is distributed over the porphyrin atoms with the highest contribution at the C_m and N_p atoms. Because the porphyrin a_{2u} orbital has a high amplitude just at these atoms, this is an indication for filling the hole in the a_{2u} orbital during the hydroxylation reaction. The main change of the effective charges of the substrate atoms with decreasing carbon–oxygen distance takes place at the carbon atom under attack (see Tables 1 and 2) which becomes significantly more positive than the other substrate carbon atoms.

The reduction of the overlap population of the Fe–O bond with decreasing C–O distance (see Tables 3 and 4) expresses the tendency towards bond breaking even though the Fe–O bond distance is kept constant. Concomitantly a new bond between the oxygen and the carbon atom under attack is formed. A small increase of the Fe–S bond strength is obtained, while variations in the overlap population of the other bonds within the porphyrin core are negligible. A slight increase of the C_1–N bond strength is observed during the reaction since the substrate orbital participating in the electron transfer process has anti-bonding character with respect to this bond. The ionic contribution to the bond remains nearly unchanged because the increase of the positive carbon charge (C_1) is compensated by the decrease of the negative charge of N.

In the substrate-free Por^+ Fe(IV)O cation radical complex the two impaired electrons in the Fe–O subunit are markedly delocalized towards the oxygen compared with the expectation from ligand field theory. This effect diminishes during the hydroxylation reaction, i.e. the spin density in the O(2p) orbitals is reduced while the Fe(3d) spin density increases indicating the initial step to the formation of Fe(III) (see Tables 5 and 6). These changes as well as the change in the S(3p) spin density are more pronounced than the corresponding changes in the hydroxylation of fluorobenzene [1]. The decrease of spin density at N_p, corresponds to the gradual population of the spin-down a_{2u} orbital. The spin density of 0.64 induced in the substrate at the maximum of the potential curve (*para* hydroxylation) is higher than in the case of fluorobenzene [1], so that the substrate has slightly more radical character. The

Table 5
Changes of spin densities for the reaction of 3-fluoro-6-methylaniline with the cysteinate-type coordinated $Por^{+}Fe(IV)O$ cation radical complex (attack on *para*-position with respect to NH_2)

r_{OC}	Fe(3d)	N_3(2p)	S(3p)	O(2p)	C_{135}[b](2p)	C_4(2p)	N_a(2p)	F(2p)	Sub[c]
inf[a]	1.2398	0.0756	0.1264	0.8767	—	—	—	—	
2.450	1.312	0.068	0.207	0.838	0.041	0.021	0.006	0.002	0.073
2.356	1.317	0.065	0.214	0.813	0.063	0.026	0.008	0.002	0.103
2.260	1.330	0.061	0.220	0.777	0.096	0.031	0.011	0.004	0.145
2.167	1.368	0.053	0.224	0.725	0.146	0.033	0.016	0.005	0.201
2.074	1.422	0.042	0.229	0.653	0.218	0.033	0.022	0.007	0.280
1.981	1.487	0.028	0.236	0.557	0.323	0.027	0.031	0.011	0.387
1.890	1.555	0.014	0.243	0.446	0.451	0.018	0.040	0.014	0.514
1.800	1.609	0.001	0.250	0.335	0.581	0.006	0.049	0.018	0.638
1.710	1.646	−0.007	0.260	0.242	0.671	−0.005	0.053	0.020	0.721
1.622	1.686	−0.010	0.275	0.171	0.707	−0.013	0.053	0.020	0.748
1.535	1.738	−0.005	0.295	0.118	0.699	−0.016	0.051	0.020	0.736

[a] Separated systems with deformed structures (see text).
[b] 2p Spin density of C_1, C_3 and C_5 atoms of the substrate.
[c] Spin density of the substrate.

induced spin is almost exclusively located at the carbon atoms next and opposite to the site of attack. This is caused by the expected decrease of the spin-down charge density in the p_z and p_x atomic orbitals, but also by an increased spin-up density in the p_z and p_x atomic orbitals, so that the change in the spin density of the substrate is predominantly a polarization effect.

The corresponding results for the charge and spin redistribution during the reaction as well as for the energies and character of the spin-down orbitals (the latter being discussed below) involved in the hydroxylation reaction at the *para* position for the porphyrin with the shorter Fe–N distance of 200 pm reveal the same trends and are available as supplementary material (Tables S1, S2, S3, S4 and Fig. S2). For this reason the subsequent discussion will be restricted to the model system with a Fe–N bond distance of 204 pm.

Table 6
Changes of spin densities for the reaction of 3-fluoro-6-methylaniline with the cysteinate-type coordinated $Por^{+}Fe(IV)O$ cation radical complex (attack on *ortho*-position with respect to NH_2)

r_{OC}	Fe(3d)	N_p(2p)	S(3p)	O(2p)	C_{135}[b](2p)	C_2(2p)	N_a(2p)	F(2p)	Sub[c]
inf[a]	1.2398	0.0756	0.1264	0.8767	—	—	—	—	—
2.449	1.324	0.067	0.207	0.827	0.042	0.024	0.008	0.002	0.095
2.356	1.329	0.064	0.214	0.801	0.065	0.030	0.011	0.002	0.100
2.260	1.344	0.059	0.221	0.764	0.099	0.035	0.015	0.004	0.150
2.167	1.381	0.052	0.225	0.712	0.148	0.038	0.020	0.005	0.209
2.074	1.432	0.042	0.230	0.639	0.217	0.037	0.024	0.007	0.282
1.981	1.500	0.028	0.238	0.543	0.320	0.032	0.032	0.011	0.386
1.890	1.570	0.013	0.245	0.433	0.447	0.022	0.040	0.015	0.511
1.800	1.628	0.001	0.253	0.324	0.573	0.009	0.047	0.019	0.631
1.710	1.670	−0.007	0.262	0.235	0.661	−0.003	0.050	0.021	0.710
1.622	1.711	−0.011	0.273	0.167	0.698	−0.011	0.049	0.022	0.739
1.535	1.764	−0.014	0.292	0.114	0.691	−0.015	0.046	0.021	0.743

[a] Separated systems with deformed structures (see text).
[b] 2p Spin density of C_1, C_3 and C_5 atoms of the substrate.
[c] Spin density of the substrate.

4.2. Orbital interactions

A more detailed insight into the reaction process can be obtained by analysing the changes in character and energy of the molecular orbitals involved in the reaction. For this purpose only the spin-down orbitals constituting the HOMOs (highest occupied molecular orbitals) and LUMOs (lowest occupied molecular orbitals) of the interacting system, have to be considered. Analogous changes in character within the interacting spin-up orbitals do not influence the total energy because they are occupied.

The HOMO of the non-deformed gas-phase 3-fluoro-6-methylaniline molecule is a combination of p_z-orbitals with participation mainly of N (25%), C_4 (20%), C_6 (18%) and C_1 (16%). This orbital has antibonding character with respect to the C–N and C–F bonds. The HOMO of the deformed substrate has an increased participation from the C atom where the deformation takes place, namely 39% (C_4) and 35% (C_2) for the *para*- and *ortho*-position, respectively. This favours the electrophilic attack on this C atom by the oxo group of the $Por^+Fe(IV)O$ cation radical complex.

The electron flow from the substrate towards the porphyrin should stabilize the substrate orbitals and destabilize the porphyrin orbitals. However, only the porphyrin a_{1u}-orbital (MO no. 90), the Fe($3d_{xy}$)-orbital (MO no. 91) and the Fe($3d_{x^2-y^2}$)-orbital (MO no. 96) follow this expectation, since they do not participate in the reaction. In contrast, the ordering of the orbitals directly involved in the reaction is determined by other factors.

Five orbitals are involved in the hydroxylation reaction at both *para*- and *ortho*-position (cf. Tables 7 and 8 and Walsh diagrams — Fig. 4a,b). At large separation, $r_{OC} = 245$ pm, these are the

Table 7
Energies (in eV) and character (in percent) of the spin-down orbitals involved in the reaction of 3-fluoro-6-methylaniline with the cysteinate-type $Por^+Fe(IV)O$ cation radical complex (attack on *para*-position with respect to NH_2)

r_{OC}	ϵ_{89}	b	O	Fe	S	a_{2u}	ϵ_{92}	b	O	Fe	S	a_{2u}
2.449	−7.51	42	10	18	6	7	−7.11	1	15	4	56	15
2.356	−7.46	34	8	18	7	8	−7.08	2	15	3	55	17
2.260	−7.39	28	6	17	8	9	−7.06	3	14	3	53	20
2.167	−7.33	28	5	20	14	12	−7.04	4	13	3	48	24
2.074	−7.27	22	4	21	22	13	−7.02	8	10	6	29	30
1.981	−7.23	11	3	20	34	11	−6.98	12	8	7	28	43
1.890	−7.23	3	2	15	35	6	−6.93	12	4	8	15	54
1.800	−7.24	1	3	19	50	8	−6.87	8	1	11	10	64
1.710	−7.26	0	3	19	52	8	−6.84	4	1	13	7	70
1.622	−7.26	0	3	20	52	8	−6.83	2	1	15	6	72
1.535	−7.26	0	2	20	52	7	−6.81	1	0	15	1	73

r_{OC}	ϵ_{93}	b	O	Fe	S	a_{2u}	ϵ_{94}[a]	b	O	Fe	S	ϵ_{95}[a]	b	O	Fe	S
2.449	−7.03	6	5	4	17	63	−6.34	0	42	56	0	−6.24	2	33	55	9
2.356	−6.98	8	6	3	18	62	−6.32	0	40	57	0	−6.22	4	31	55	9
2.260	−6.93	11	6	2	18	59	−6.30	1	38	59	0	−6.20	5	29	55	9
2.167	−6.87	14	6	3	18	54	−6.32	1	36	61	0	−6.20	8	27	54	9
2.074	−6.80	18	6	5	17	47	−6.37	2	32	63	0	−6.23	14	24	52	10
1.981	−6.73	20	6	12	17	39	−6.44	3	28	65	1	−6.28	21	20	46	10
1.890	−6.67	14	5	28	17	29	−6.52	4	22	66	4	−6.30	37	16	33	7
1.800	−6.67	2	12	56	9	17	−6.56	5	12	59	16	−6.24	59	11	15	4
1.710	−6.70	0	13	67	4	13	−6.58	1	7	59	13	−6.10	71	6	7	3
1.622	−6.72	0	11	69	2	13	−6.59	0	6	61	25	−5.92	76	3	6	3
1.535	−6.73	0	9	71	2	13	−6.58	0	4	62	27	−5.78	76	1	6	3

[a] No a_{2u} contribution in this orbital.

Table 8
Energies (in eV) and character (in percent) of the spin-down orbitals involved in the reaction of 3-fluoro-6-methylaniline with the cysteinate-type $Por^+Fe(IV)O$ cation radical complex (attack on *ortho*-position with respect to NH_2)

r_{OC}	ϵ_{89}	b	O	Fe	S	a_{2u}	ϵ_{92}	b	O	Fe	S	a_{2u}
2.449	−7.51	43	9	18	7	7	−7.11	1	15	4	56	15
2.356	−7.45	38	8	19	9	9	−7.08	1	14	3	55	18
2.260	−7.39	33	7	20	11	11	−7.06	3	14	2	52	21
2.167	−7.33	29	5	21	16	13	−7.04	5	12	3	47	25
2.074	−7.31	21	3	21	25	13	−7.01	8	10	6	38	31
1.981	−7.24	10	3	20	37	11	−6.99	12	7	6	27	45
1.890	−7.23	4	3	20	46	8	−6.92	11	3	8	15	55
1.800	−7.24	1	3	20	51	8	−6.86	8	1	10	10	65
1.710	−7.26	0	2	20	53	8	−6.83	4	1	12	8	71
1.622	−7.27	0	2	20	53	8	−6.81	2	1	13	7	73
1.535	−7.26	0	2	20	53	8	−6.79	1	1	13	6	75

r_{OC}	ϵ_{93}	b	O	Fe	S	a_{2u}	ϵ_{94}[a]	b	O	Fe	S	ϵ_{95}[a]	b	O	Fe	S
2.449	−7.02	6	5	4	17	63	−6.33	0	41	56	0	−6.24	3	32	55	9
2.356	−6.97	8	6	3	18	61	−6.30	0	40	58	0	−6.21	4	31	55	9
2.260	−6.91	12	6	2	18	58	−6.29	0	38	59	0	−6.19	6	29	55	9
2.167	−6.86	15	6	3	18	53	−6.32	0	35	62	0	−6.20	9	26	54	9
2.074	−6.79	15	6	6	17	46	−6.36	1	32	64	0	−6.22	14	23	51	9
1.981	−6.71	20	5	13	18	38	−6.44	2	27	67	1	−6.26	23	20	45	9
1.890	−6.65	14	6	29	18	28	−6.52	3	21	67	4	−6.28	40	16	31	7
1.800	−6.65	2	12	60	8	14	−6.57	3	10	58	17	−6.22	60	11	14	4
1.710	−6.69	0	14	71	2	10	−6.59	1	6	57	24	−6.07	71	6	7	3
1.622	−6.72	0	12	73	2	10	−6.59	0	5	59	26	−5.89	76	3	6	3
1.535	−6.73	0	9	74	1	10	−6.58	0	4	60	27	−5.75	77	1	6	3

[a] No a_{2u} contribution in this orbital.

highest occupied p_z, bonding substrate orbital (denoted as b in the Tables and Figures) containing approx. 25% admixture from the bonding π_x(Fe–O)-orbital (denoted by Fe and O), the S(3p)-lone-pair-orbital (denoted as S), the porphyrin a_{2u}-orbital, constituting the LUMO of the whole system, and the antibonding π_y^*(Fe–O)- and π_x^*(Fe–O)-orbitals.

When the substrate approaches the $[PorFe(IV)O]^+$ cation radical complex, the substrate orbital b undergoes a strong destabilization from MO no. 89 to MO no. 95, so that it becomes unoccupied in the course of the reaction. Simultaneously, MO no. 89 is transformed into a bonding $Fe(3d_{xz})$–$S(3p_x)$ orbital, and the former S(3p)-lone-pair-orbital (HOMO) transforms into a_{2u} along the reaction pathway with an Fe–S antibonding participation of approx. 20% at the maximum of the potential curve. For large substrate–porphyrin separations the LUMO (MO no.93) of the interacting system is the porphyrin a_{2u}-orbital, but looses the a_{2u}-character for short C–O distances. Temporarily, the contribution from the substrate orbital b to the LUMO increases, but vanishes at the maximum of the potential curve, and the LUMO is transformed into an antibonding π_y^*(Fe–O) orbital with a small π_y^*(Fe–S) contribution. The MO no. 94 [π_y^*(Fe–O) at large separations] changes to a predominantly Fe(3d)-orbital with small participations from the π_x^*(Fe–S) and π_x^*(Fe–O) antibonding orbitals. Finally, the Mo no. 95 changes from a π_x^*(Fe–O) orbital to the substrate b-orbital with a small antibonding π_x^*(Fe–O) participation.

This analysis of the orbital interactions concerns both hydroxylation at *para*- and *ortho*-positions and reveals the electron flow as taking place from the substrate b orbital to the porphyrin a_{2u}-orbital. It is accompanied by an additional electron delocalization along the axial ligands ex-

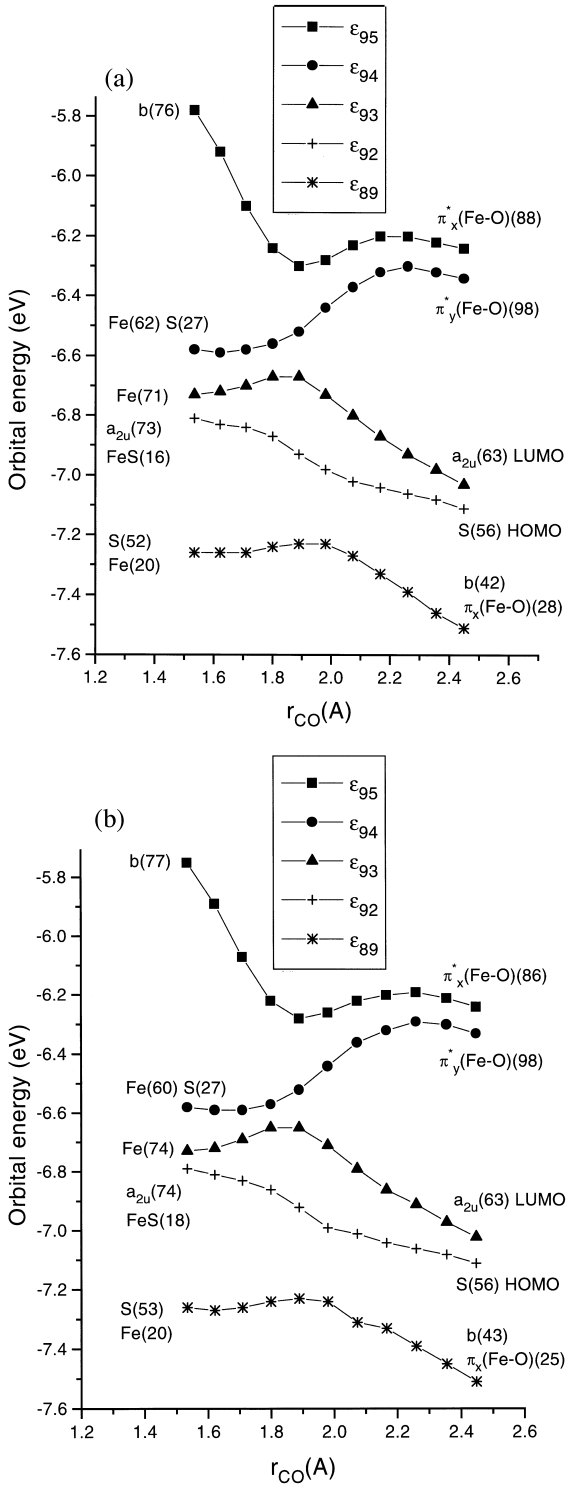

Fig. 4.

pressed by the transformation of the π(Fe–O) orbitals into π(Fe–S) orbitals. Concomitantly, the S(3p) atomic orbitals participate along the reaction coordinate in all molecular orbitals involved in the hydroxylation process. In this sense the S(3p)-lone-pair orbital facilitates the reaction. It transforms into a_{2u} and, thus, causes the electron flow to the porphyrin. At the same time, the π_x^*(Fe–O)-orbital is transformed into the substrate b orbital and plays the role of an electron mediator. Altogether the orbital interactions taking place during the reaction demonstrate that the weakening of the Fe–O bond is due to a polarization-delocalization effect, while the Fe–S bond strength remains approximately the same because the antibonding Fe–S participation in the HOMO nearly compensates the effect of the transformation of the Fe–O bond into the Fe–S bond.

5. Conclusions

The reaction mechanism for the hydroxylation of 3-fluoro-6-methylaniline, attacked at different positions (epoxide formation and direct attack at the positions *para* and *ortho* with respect to the NH_2 group as a primary reaction step) as well as the epoxide formation for 3-fluoroaniline catalysed by a $[PorFe(IV)O]^+$ a_{2u}-cation radical complex have been investigated on the basis of electronic structure calculations in local spin-density approximation.

Potential curves with different geometrical orientations of the substrate with respect to the ferryl-oxo porphyrin cation radical complex have been calculated in order to find those arrangements which enable the primary reaction step. The subsequent results about the reaction pathway and the reaction mechanism have been obtained.

Fig. 4. Walsh diagram of the five interacting spin-down molecular orbitals of the substrate–porphyrin system for the hydroxylation at the *para*-position (a) and at the *ortho*-position (b) as a function of the C–O distance. MO no. 90 (the porphyrin a_{1u} orbital) and no. 91 [($Fe(3d_{xy})$ orbital] are not shown because they are not involved in the reaction.

1. Non-repulsive potential curves exist only in cases of direct attack at the *para*- and the *ortho*-positions with respect to NH_2, but not for epoxide formation as a primary reaction step.
2. The preferential orientation enabling the reaction in cases of direct attack at the *para*- and *ortho*-positions is determined by repulsive interactions between the substituents of the substrate and the porphyrin and not by the porphyrin–substrate dipole–dipole interactions which turns out to be rather unfavourable. Unlike as in case of the hydroxylation of monofluorobenzene, the substrate plane is not parallel to the porphyrin plane and the orientation of the substrate is different in both cases, which emphasizes the significance of the substituents of the substrate.
3. Hydroxylation at the *para*-position is more likely than at the *ortho*-position as can be derived from comparing total energies, the relative heights of the energy barriers and the C–O distances where the interactions become attractive in both cases. This is ill accordance with results of the in vivo biotransformation of 3-fluoro-6-methylaniline into aromatic ring hydroxylated products by cytochrome P450.
4. The hydroxylation reaction consists of three parts, namely a partial electron transfer from the HOMO of the substrate into the empty a_{2u}-orbital of the porphyrin, weakening of the Fe–O bond leading eventually to bond rupture, and the formation of the C–O bond. The Fe–O bond rupture is mainly caused by the electron flow from the Fe–O bond into the Fe–S bond. The Fe–S bond strength, however, remains approximately the same because the electron flow into the Fe–S bond is almost compensated by the population of the antibonding Fe–S orbital participating in the HOMO of the reaction product.
5. The reduction of the Fe–N distance from 204 pm to 200 pm (hydroxylation at the *para*-position) does not change the general characteristics of the reaction and has virtually no influence on the energies and the changes in the character of the orbitals involved in the reaction.
6. The decisive role played by sulphur in the hydroxylation reaction is obvious from the participation of the S(3p)-orbitals in all molecular orbitals involved in the reaction.
7. The change in the spin density of the substrate is predominantly a polarization effect.

The amounts of charge- and spin-density induced in the substrate along the reaction pathway reveal that the reaction intermediates may be described as somewhere between the radical and cation σ-adducts.

Acknowledgements

We gratefully acknowledge support from the EU Human Capital and Mobility grant to the MASIMO network (ERBCHRX-CT-920072), and from Biotech grant no. BIO2CT942052.

References

[1] O. Zakharieva, M. Grodzicki, A.X. Trautwein, C. Veeger, I.M.C.M. Rietjens, Biol. Inorg. Chem. 1 (1996) 192–204.
[2] K.R. Korzekwa, W.F. Trager, M. Gouterman, D. Spangler, G.H. Loew, J. Am. Chem. Soc. 107 (1985) 4273–4279.
[3] K.R. Korzekwa, D.C. Swinney, W.F. Trager, Biochemistry 28 (1989) 9019–9027.
[4] J. Vervoort, I.M.C.M. Rietjens, W.J.H. van Berkel, C. Veeger, Eur. J. Biochem. 206 (1992) 479–484.
[5] I.M.C.M. Rietjens, A.E.M.F. Soffers, C. Veeger, J. Vervoort, Biochemistry 32 (1993) 4801–4812.
[6] P.R. Ortiz de Montellano (Ed.), Oxygen activation and transfer, in: Cytochrome P-450: Structure, Mechanism and Biochemistry, Plenum Press, New York, 1986, pp. 217–271.
[7] F.P. Guengerich, T.L. MacDonald, FASEB J 4 (1990) 2453.
[8] P. Du, G. Loew, Int. J. Quant. Chem. 44 (1992) 251–261.
[9] J. Koerts, S.J. Boeren, J. Vervoort, R. Weiss, C. Veeger, I.M.C.M. Rietjens, Chem. Biol. Interact. 1996, p. 99.
[10] N.H.P. Cnubben, J. Vervoort, C. Veeger, I.M.C.M. Rietjens, Chem.-Biol. Interact. 85 (1992) 151–172.
[11] O.S. Son, D.W. Everett, E.S. Fiala, Xenobiotica 10 (1980) 457–468.
[12] J.W. Daly, G. Guroff, S. Udenfriend, B. Witkop, Biochem. Pharmacol. 17 (1968) 31–36.
[13] K.L. Cheever, D.E. Richards, H.B. Plotnic, Toxicol. Appl. Pharmacol. 56 (1980) 361–369.

[14] K.E. Wade, J. Troke, C.M. MacDonald, I.D. Wilson, J.K. Nicholson, Bioanalysis of Drugs and Metabolites, E. Reid, J.D. Robinson, I. Wilson (Eds.), Plenum Publishing Corporation, New York, 1988, pp. 383–388.
[15] S. Boeren, B. Tyrakowska, J. Vervoort, E. de Hoffman, K. Tennis, A. van Veldhuizen, I.M.C.M. Reitjens, Xenobiotica 22 (1992) 1403–1423.
[16] B. Tyrakowska, S. Boern, B. Geurtsen, I.M.C.M. Riet-Jens, Drug Metab. Dispos. 21 (1993) 508–519.
[17] A. Goldblum, G.H. Loew, J. Am. Chem. Soc. 107 (1985) 4265–4272.
[18] R.N. Armstrong, Enzyme-catalyzed detoxification reactions: mechanism and stereo chemistry. CRC Crit. Rev. Biochem. 22 (1987) 39–88.
[19] D.M. Jerina, J.W. Daly, Science 185 (1974) 573–582.
[20] J.W. Daly, D.M. Jerina, B. Witkop, Experientia 28 (1972) 1129–1264.
[21] H.G. Selander, D.M. Jerina, D.E. Piccolo, G.A. Berchtold, J. Am. Chem. Soc. 97 (1975) 4428–4430.
[22] R.P. Hanzlik, K. Hogberg, C.M. Judson, Biochemistry 23 (1984) 3048–3055.
[23] P.N. Rizk, R.P. Hanzlik, Xenobiotica 25 (1995) 143–150.
[24] M. Grodzicki, J. Phys. B 13 (1980) 2683–2692.
[25] Grodzicki, M., Theorie und Anwendung der Self-Consistent-Charge-X α Methode, Thesis of habilitation, Hamburg, 1985.
[26] D. Habibollahzadeh, M. Grodzicki, J.M. Seminaro, P. Politzer, J. Phys. Chem. 95 (1991) 7699–7702.
[27] M. Grodzicki, J.M. Seminaro, P. Politzer, J. Chem. Phys. 94 (1991) 1668–1669.
[28] M.J. Frisch et al., GAUSSIAN 90, Revision H, Gaussian Inc., Pittsburgh, PA, 1990.
[29] J. Antony, M. Grodzicki, A.X. Trautwein, J. Phys. Chem. A 101 (1997) 2692–2701.
[30] B.M.L. Chen, A. Tulinsky, J. Am. Chem. Soc. 94 (1972) 4144–4151.
[31] M. Schappacher, R. Weiss, R. Montiel-Montoya, A. Trautwein, A. Tabard, J. Am. Chem. Soc. 107 (1985) 3736–3738.
[32] L.A. Andersson, J.H. Dawson, Struct. Bonding 74 (1990) 1–40.
[33] K.G. Ravichandran, S.S. Boddupalli, C.A. Hasemann, J.A. Peterson, J. Deisenhofer, Science 261 (1993) 731–736.
[34] J.P. Dahl, J. Avery (Eds.), Local Density Approximations in Quantum Chemistry and Solid State Physics, Plenum Press, New York and London, 1984.
[35] R.G. Parr, W. Yang, Density-Functional Theory of Atoms and Molecules, Oxford University Press, New York, 1989.
[36] J.K. Labanowski, J.W. Andzelm (Eds.), Density Functional Methods in Chemistry, Springer, New York, Berlin, Heidelberg, 1991.
[37] H. Paulsen, X.-Q. Ding, M. Grodzicki, Ch. Butzlaff, A.X. Trautwein, R. Hastung, K. Wieghardt, Chem. Phys. 184 (1994) 149–162.
[38] H. Paulsen, M. Kröckel, M. Grodzicki, E. Bill, A.X. Trautwein, G.L. Leigh, H. Paulsen, J. Inorg. Chem. 34 (1995) 6244–6249.
[39] M. Grodzicki, H. Flint, H. Winkler, F.A. Walker, A.X. Trautwein, J. Phys. Chem. A 101 (1997) 4202–4207.
[40] B.D. Preston, J.A. Miller, E.C. Miller, J. Biol. Chem. 258 (1983) 8304–8311.
[41] J.E. Tomaszewski, D.M. Jerina, J.W. Daly, Biochemistry 14 (1975) 2024–2031.